KfK 3798
Oktober 1984

The Optical Potential for ^{6}Li-^{6}Li Elastic Scattering at 156 MeV

S. Micek, Z. Majka, H. Rebel, H. J. Gils, H. Klewe-Nebenius
Institut für Kernphysik

Kernforschungszentrum Karlsruhe

Kernforschungszentrum Karlsruhe
Institut für Kernphysik

KfK 3798

THE OPTICAL POTENTIAL FOR ^{6}Li-^{6}Li ELASTIC SCATTERING AT 156 MeV

S. Micek[+], Z. Majka[+]
H. Rebel, H.J. Gils, H. Klewe-Nebenius[++]

[+] Institute of Physics, Jagellonian University, Cracow, Poland
[++] Institut für Radiochemie

Kernforschungszentrum Karlsruhe GmbH, Karlsruhe

Kernforschungszentrum Karlsruhe GmbH
ISSN 0303-4003

Abstract:

Elastic scattering of ^{6}Li from ^{6}Li has been studied for the beam energy of 156 MeV. The experimental differential cross section has been analysed on the basis of the optical model using various phenomenological forms. The spin-orbit interaction proves to be less significant. A semi-microscopic double-folding cluster model which generates the real part of the optical potential by an antisymmetrized d-α cluster wave function of ^{6}Li and α-α, d-d and d-α interactions is well able to describe the experimental data.

DAS OPTISCHE POTENTIAL FÜR DIE ELASTISCHE STREUUNG VON ^{6}Li-IONEN AN ^{6}Li BEI 156 MeV

Die elastische Streuung von ^{6}Li an ^{6}Li wurde bei einer Strahlenergie von 156 MeV untersucht. Der experimentelle differentielle Wirkungsquerschnitt wurde im Rahmen des optischen Modells mit verschiedenen phänomenologischen Formen ausgewertet. Die Spin-Bahn-Wechselwirkung erweist sich als wenig signifikant. Ein halbmikroskopisches Doppelfaltungs-Cluster-Modell, das den Realteil des optischen Potentials mit einer antisymmetrischen d-α-Clusterwellenfunktion von ^{6}Li und α-α, d-d und d-α - Wechselwirkungen erzeugt, beschreibt die experimentellen Daten recht gut.

1. Introduction

The investigation of elastic scattering of ^{6}Li projectiles is of considerable interest as there is a change in the character of elastic scattering observed in the transition from light to heavy ions. At higher bombarding energies and light target nuclei nuclear rainbow scattering has been observed, a feature, which is experimentally established for ^{6}Li scattering from ^{12}C [1] and ^{28}Si [2] and has been found to lead to an increased sensitivity to the shape of the interaction potential. Current microscopic interpretations of the scattering of complex nuclear particles generate the optical potential, in particular its real part, by folding a realistic effective G-matrix interaction with the projectile and target density distributions. These "double-folding" procedures have generally been found to be successful in reproducing elastic scattering angular distributions for light and heavy ions [3]. The only projectiles whose scattering cross sections could not be described by such an approach are Li and Be. They appear to be anomalous in the sense that the strength of the double-folding potentials have to be reduced by factors of about 0.5 in order to reproduce the measured differential cross sections. In the case of ^{7}Li and ^{9}Be scattering this anomaly has been tentatively ascribed to strong effects of quadrupole scattering [4]. However, since ^{6}Li has a very small quadrupole moment, the observed feature still presents a problem. Another possible explanation is based on projectile breakup effects in the elastic channel [5]. Indeed, Sakuragi et al [6] could well describe elastic scattering [7] of 156 MeV ^{6}Li from ^{40}Ca by including a discretized breakup continuum of ^{6}Li into the coupled channel calculations. Alternatively, cluster structure effects originating from the projectile [8] and from both the projectile and the target nucleus [9] have been incorporated into the double-folding approach. In the double-folding cluster model [9] the real part of the optical potential for ^{6}Li scattering is generated with phenomenological d-α and α-α interactions and internal cluster wave functions. This approach has been shown to describe the ^{6}Li + ^{12}C scattering data at 156 MeV as well as the phenomenological optical potential with conventional radial forms, and significantly better than the usual double-folding model. It appears to be rather in-

teresting that the cluster structure even of the target nucleus seems to affect the interaction potential. The question to which extent such effects may be evident in a scattering system of highly clusterized complex particles has prompted us to study the elastic scattering of ^{6}Li from ^{6}Li. This symmetric system has already been investigated at rather low beam energies [10] where elastic scattering only probes the outermost part of the potential, so that conclusions are difficult, and where even the concept of a local optical potential is doubtful. The present paper presents the experimental cross sections for the ^{6}Li + ^{6}Li case at a projectile energy E_{Li} = 156 MeV. The analysis of the data attempts to explore the radial shape and the microscopic structure of the interaction potential.

2. Experiment

The experimental basis of our studies are measurements of the differential cross sections for the scattering of 156 MeV ^{6}Li ions from ^{6}Li targets (isotopically enriched to 99.0 % and with a thickness of ca. 3 mg/cm^2). The measurements have been performed at the Karlsruhe Isochronous Cyclotron and are part of a more detailed investigation [11] of nuclear reactions induced by ^{6}Li projectiles bombarding ^{6}Li. The experimental procedures applied in the scattering studies are very similar to previous investigations (given in Ref. 12). Fig. 1 displays some energy spectra of scattered ^{6}Li particles measured with a ΔE-E Si surface barrier detector telescope, showing also the excitation of the first excited state ($I^{\pi} = 3^{+}_{1}$) and the double excitation of ^{6}Li. In addition to discrete peaks a broader bump is observed, well pronounced at forward angles, which can be ascribed to quasi-elastic scattering from the α-particle cluster with a deuteron spectator; the theoretical curves in Fig. 1 indicate simple PWBA predictions of such a mechanism, [11] not discussed further.

In the present paper we are mainly interested in elastic scattering. The experimental differential cross sections are shown together with results of the optical model analyses in Fig. 24.

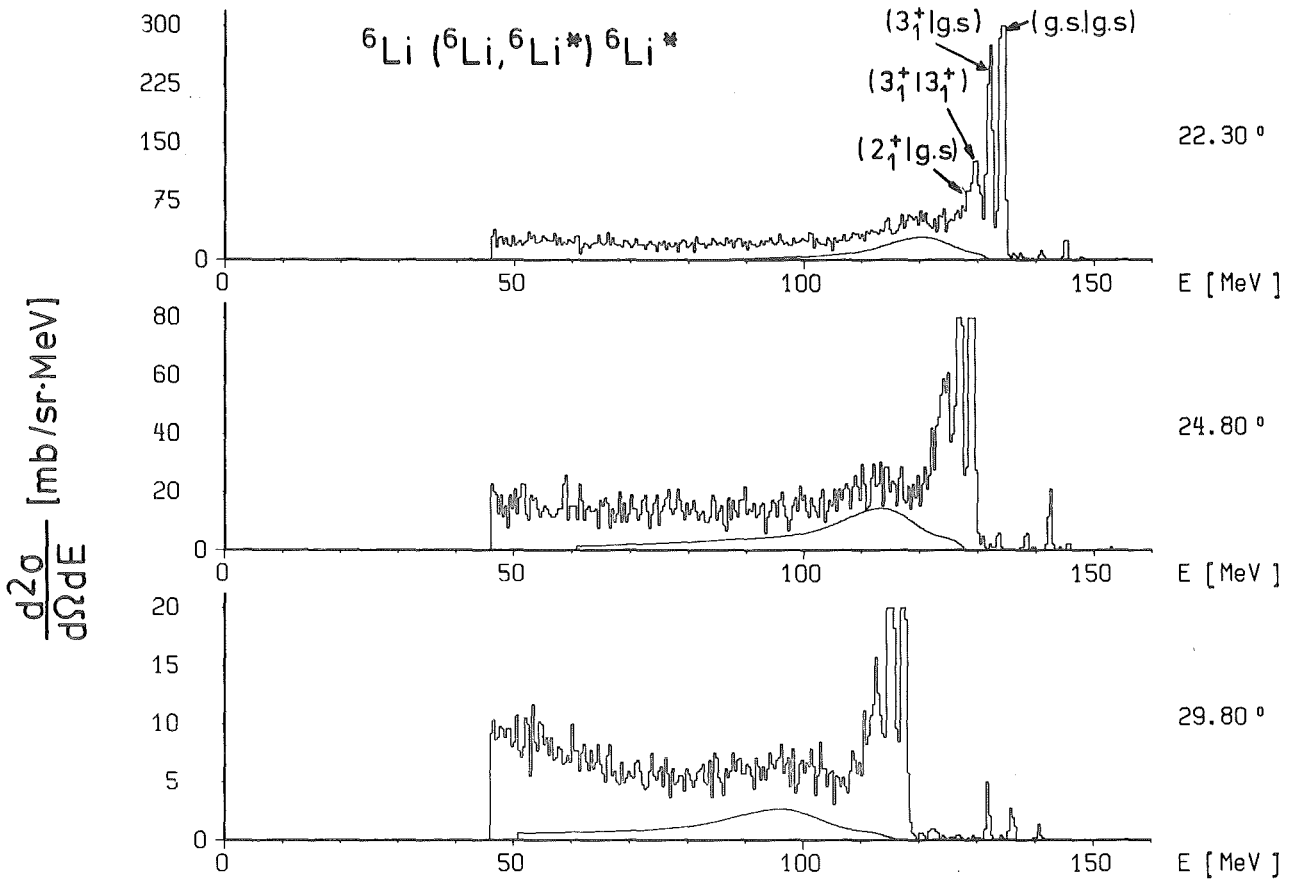

Fig. 1 Energy spectra of scattered ^{6}Li particles from ^{6}Li showing mutual excitation and quasi-free scattering contributions.

3. Phenomenological optical potentials

In order to study how well phenomenological optical potentials describe the experimental data and to look for possible effects originating from a spin-orbit interaction, the experimental differential cross sections have been initially analysed on the basis of various phenomenological forms (Woods-Saxon and squared Wood-Saxon form factors) of the real potential using volume (Woods-Saxon form: W_o, r_w, a_w) and surface absorption (W_s, r_s, a_s). The Coulomb potential was assumed to be due to a uniformly charged sphere of the radius $R_c = 1.5\ (A_T^{1/3} + A_P^{1/3})$ fm. A standard optical model code has been altered to include Bose-Einstein statistics of identical particles with spin 1. In principle, a spin-orbit interaction is involved in the scattering process, coupling the spin

of each ^{6}Li nucleus to the relative orbital angular momentum. Microscopic considerations [7] suggest an $1/A_P$ dependence of the spin-orbit potential, so that a rather weak potential is expected, as the ^{3}He spin orbit potential is found to be small [13]. In fact, the present data of scattering of unpolarized ^{6}Li projectiles do not show pronounced effects due to a spin-orbit interaction.

The spin-orbit interaction has been studied in the form

$$U_{so} = v_{so}(r)\ \vec{L} \cdot \vec{S} \tag{3.1}$$

where $\vec{S} = \vec{I}_T + \vec{I}_P$ is the channel spin. The potential commutes with $\vec{S}$ so that the eigenvalues S are good quantum numbers. For ^{6}Li + ^{6}Li scattering ($I_{Li} = 1$) there are three channel-spins (S = 0,1,2), and the cross section amplitudes $f_S(\Theta)$ add incoherently

$$\begin{aligned} 2\,\frac{d\sigma}{d\Omega} = {} & \frac{1}{9}\left|f_{S=0}(\Theta) + f_{S=0}(\pi-\Theta)\right|^2 \\ & + \frac{3}{9}\left|f_{S=1}(\Theta) - f_{S=1}(\pi-\Theta)\right|^2 \\ & + \frac{5}{9}\left|f_{S=2}(\Theta) + f_{S=2}(\pi-\Theta)\right|^2 \end{aligned} \tag{3.2}$$

The radial shape $v_{so}(r)$ is chosen to be a real Thomas form

$$v_{so}(r) = V_{so} \cdot \frac{\lambda_\pi^2}{r}\ \frac{d}{dr}\ \left(1 + \exp[(r - r_{so}A_T^{1/3})/a_{so}]\right)^{-1} \tag{3.3}$$

Tab. 1 presents the parameter values of the best fit optical potentials obtained with the various forms. The inclusion of the spin-orbit potential did not improve the fits significantly. Fig. 2 displays the resulting differential cross sections (Set D), together with the partial cross sections (including their statistical weights) for the three channel spins. In the case of a vanishing spin-orbit force, 1/5 of the S=2 partial cross section equals the S=0 partial cross section which is, of course, not affected by the spin-orbit potential. The influence of a spin-orbit potential on the angular distribution is shown in Fig. 3 by theoretical cross sections calculated with parameter set B of Tab. 1 and different strengths of the spin-orbit force. Even though the experimental cross sections are less accurate for larger scattering angles,

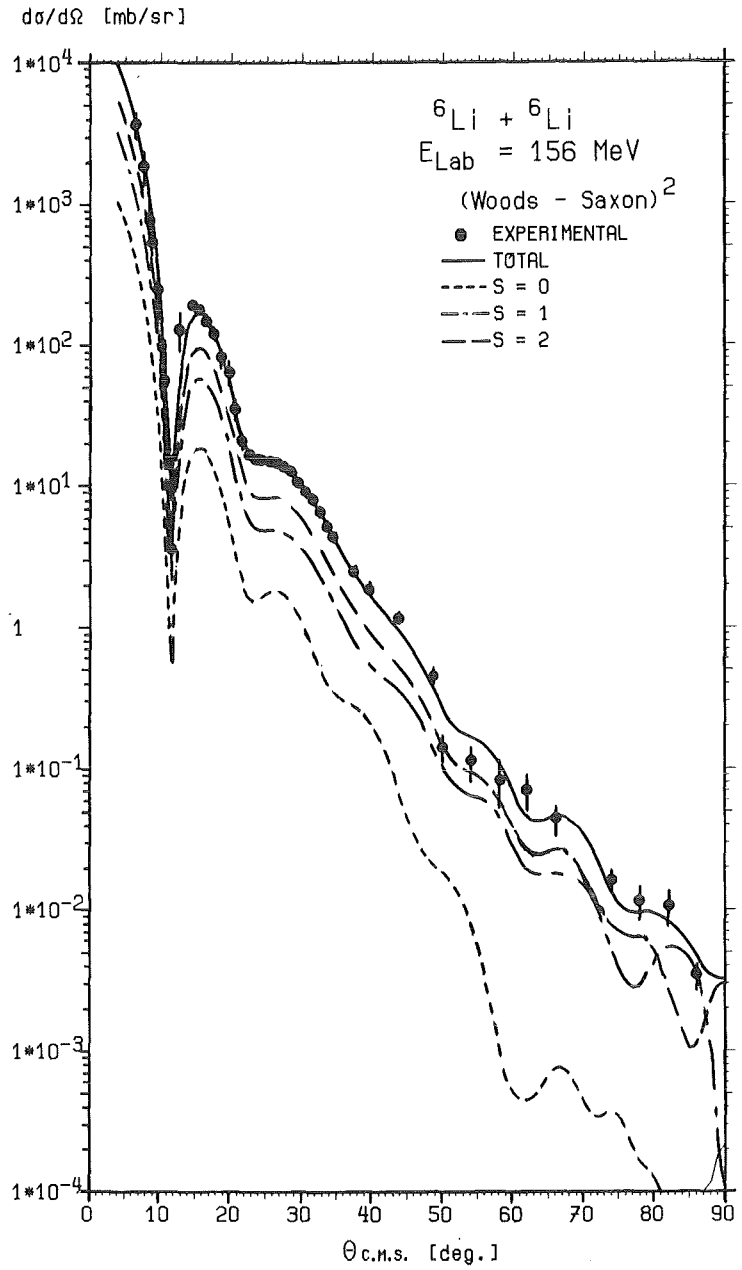

Fig. 2 Experimental differential cross sections of elastic scattering of 156 MeV ^{6}Li ions from ^{6}Li compared to the result of the optical model analysis based on a WS 2 form factor of the real potential with volume and surface absorption (Set D in Tab. 1).

they exclude a pronounced oscillation pattern as it would be for a significant spin-orbit strength.

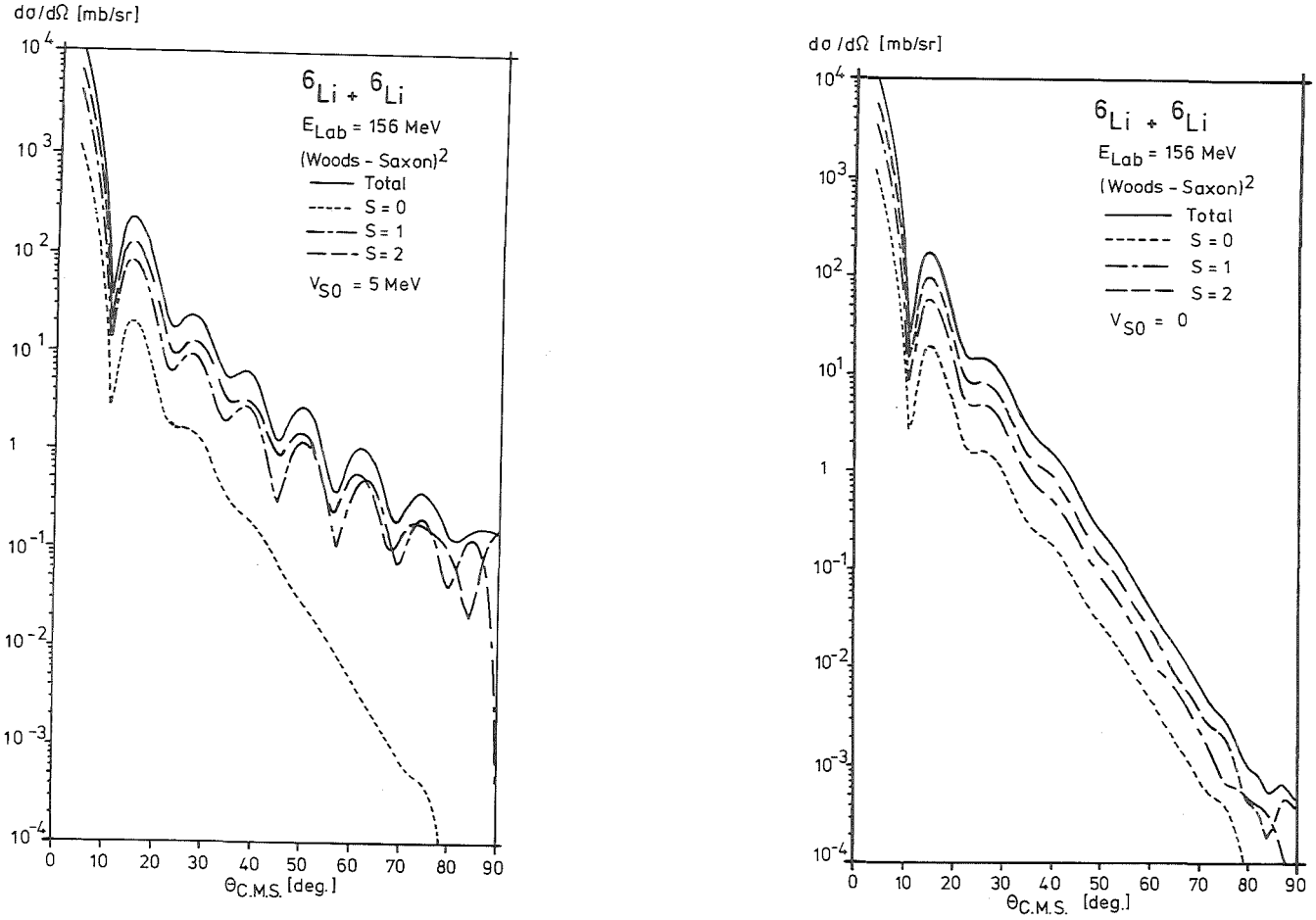

Fig. 3 Elastic scattering of 156 MeV ^{6}Li ions on ^{6}Li: Total and partial differential cross sections of the three channel-spin states calculated (with parameter set B of Tab. 1) for different strengths of the spin-orbit potential.

Real Formfactor	WS n=1	WS 2 n= 2	WS 2 n= 2	WS 2 n= 2	FB
$-V_o$ [MeV]	59.6	88.6	73.3	80.4	N=8-11
r_v [fm]	1.66	1.84	2.16	1.96	R_c=8-11fm
a_v [fm]	0.85	1.46	1.13	1.27	
$-W_o$ [MeV]	7.14	6.68	1.1	3.91	1.1
r_w [fm]	3.12	3.23	3.57	3.51	3.97
a_w [fm]	0.77	0.70	0.43	0.51	0.43
$-W_s$ [MeV]	-	-	10.7	5.3	10.7
r_s [fm]	-	-	2.10	2.00	2.11
a_s [fm]	-	-	0.58	0.53	0.58
V_{so} [MeV]	1.04	1.27	-	1.9	-
r_{so} [fm]	2.50	2.26	-	2.38	-
a_{so} [fm]	0.35	0.34	-	0.39	-
$J_v/A_p \cdot A_T$ [MeV fm^3]	340	327	374	325	385±20
χ^2/F	3.6	3.2	2.1	1.9	1.5
Set	A	B	C	D	E

Tab. 1 Phenomenological optical potential parameter values with different real form factors

$$f(r) = \left(1+\exp\left(\frac{r-r_i A_r^{1/3}}{a_i}\right)\right)^{-n}$$

The volume absorption is of the WS form, the surface absorption is parametrized by

$$U_s = 4i\, W_S\, a_s\, d/dr \left(1+\exp\left(\frac{r-r_s A_T^{1/3}}{a_s}\right)\right)^{-1}$$

The conventional radial form factors like Woods-Saxon or squared Wood-Saxon forms introduce some constraints for the radial shape of the interaction potential and obscure what is well determined and what is less determined by the data. In order to avoid such constraints we have finally applied the more model-independent Fourier-Bessel method [14] which describes the real potential by adding to a conventional form V_o an extra potential given by a Fourier-Bessel series:

$$U_R(r) = U_o(r) + \sum_{n=1}^{N} b_n j_o(q_n \cdot r) \qquad (3.4)$$

The quantities j_o are spherical Bessel functions, $q_n = n\pi/R_{cut}$, and R_{cut} is a suitable chosen cut-off radius beyond which the extra potential vanishes. The N coefficients b_n are determined by least-squares fits to the data (N = 8 - 11). Within the framework of the FB procedure the mean square uncertainty of the potential value at the distance r is given by

$$|\delta U(r)|^2 = 2 \cdot \sum_{m,n=1} \langle \delta b_m \delta b_n \rangle_{av} j_o(q_m r) j_o(q_n r), \qquad (3.5)$$

with $\langle \delta b_m \delta b_n \rangle_{av}$ being the correlation matrix between the coefficients b_n. The FB method has been shown to lead to very good values of χ^2/F and at the same time providing realistic estimates of errors [14] of the potential and its various integral quantities.

Fig. 4 displays the real $^6Li + ^6Li$ interaction potential, obtained when applying the Fourier-Bessel method and using a Woods Saxon form for the imaginary potential (see Table 1) The spin-orbit potential is ignored in the FB calculations, which rather well reproduce the experimental data. The hatched area represents the error band indicating the reduced sensitivity of the experimental cross sections to the potential at small and very large radii. The uncertainty of the resulting value of the specific volume integral $J_v/A_P A_T$ of the real central potential reflects the quality of the data. There seems to be a tendency of slightly increasing the values of $J_v/A_P A_T$ when the spin-orbit interaction is ignored in the analysis.

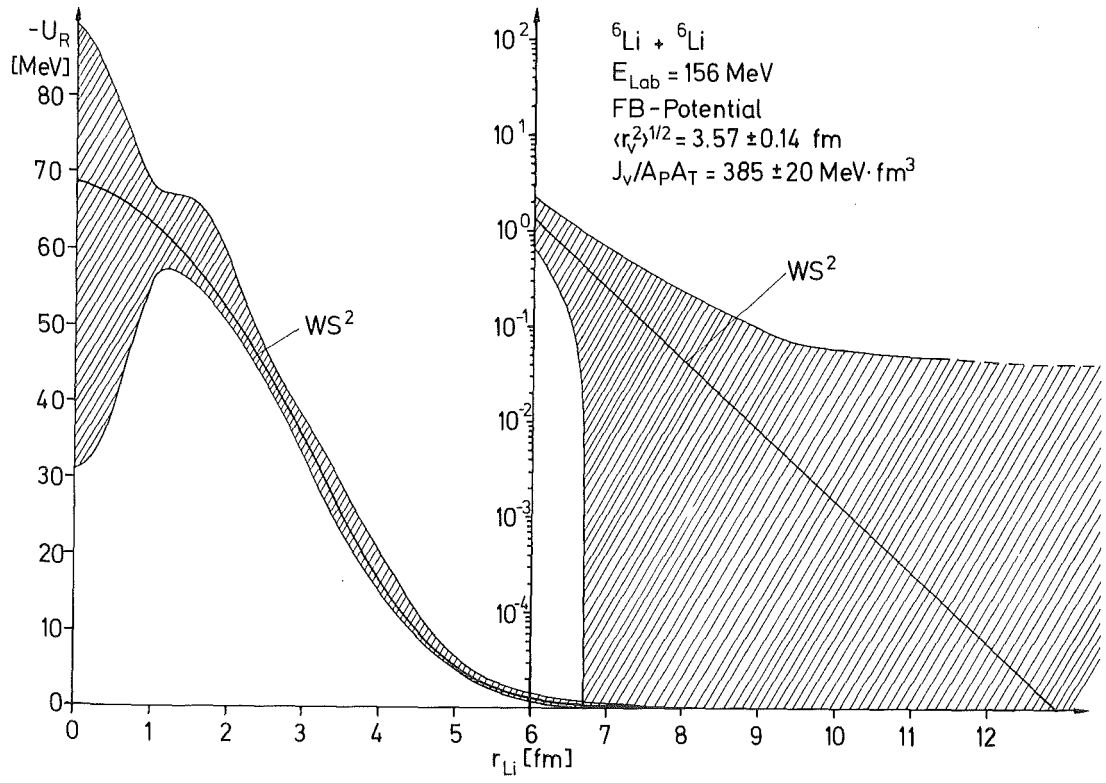

Fig. 4 Real potential for elastic scattering of 156 MeV ^{6}Li from ^{6}Li determined by the Fourier-Bessel method.

We note also that the volume of the imaginary potential proves to be rather well determined and follows the A dependence found [12] for heavier targets: $J_I/A_P A_T \approx 235 - 31\ A_T^{1/3}$ MeV · fm³.

4. Semi-microscopic approaches

In order to relate the real part of the optical potential to more basic interactions and to the structure of the colliding nuclei different semi-microscopic double folding models have been invoked and applied for the description of the present data. First, we followed the refined approach of Majka et al. [7] which has been proven rather successful in describing the elastic scattering of 156 MeV ^{6}Li from ^{40}Ca. Following ref. 7 (where details of the formulation are given) the real part of the projectile-target interaction is written as

$$U^{DF}_{LiLi}(r) = \int\int \rho^{T}_{Li}(\vec{Z}_{Li}) \cdot \rho^{P}_{Li}(\vec{Z}_{Li})\, t_{\rho}(\vec{r}_{NN}, \rho)\, d\vec{Z}^{T}_{Li}\; d\vec{Z}^{P}_{Li} \qquad (4.1)$$

with t_{ρ} being a density-dependent effective nucleon-nucleon interaction specified more in detail in ref. 7.

Actually, the indices P and T remind of the projectile and target, respectively, and ρ refers to a local density appearing in an effective nucleon-nucleon interaction

$$\rho = \rho^{P}_{Li}(Z^{P}_{Li}+r_{NN}/2) + \rho^{T}_{Li}\;(Z^{T}_{Li}+r_{NN}/2) \qquad (4.2)$$

Suggested by the results of the ^{6}Li + ^{40}Ca analysis the "sudden approximation" [7] has been used. The (point)nucleon density distribution ρ_{Li} was introduced in the form proposed by Bray et al.[15]

$$\rho_{Li}(r) = 0.203\; e^{-(0.575r)^2} + [-0.0131+0.0087(0.398r)^2]\; e^{-(0.398r)^2} \qquad (4.3)$$

Alternatively to this ordinary double-folding procedure which ignores cluster effects in the ^{6}Li structure, the real part of the optical potential has been generated by assuming a complete α-particle-deuteron clusterization in ^{6}Li. This is certainly a rather extreme assumption. However, as far as the surface of the colliding particles dominantly determines the interaction, such an assumption might better represent the density distributions entering in a double-folding calculation of the optical potential.

In this approach the real part of the potential is expressed by

$$U^{DFC}(r) = \int \{ U_{\alpha - {}^6Li}(|\vec{r} - \tfrac{1}{3}\vec{Y}|) + U_{d - {}^6Li}(|\vec{r} + \tfrac{2}{3}Y|) \} |\phi_o^{{}^6Li}(\vec{Y})|^2 \, d\vec{Y} \qquad (4.4)$$

where

$$U_{\alpha - {}^6Li}(R_\alpha) = \int \{ U_{\alpha\alpha}(|\vec{R}_\alpha - \tfrac{1}{3}\vec{Z}|) + U_{\alpha - d}(|\vec{R}_\alpha + \tfrac{2}{3}\vec{Z}|) \} |\phi_o^{{}^6Li}(\vec{Z})|^2 \, d\vec{Z} \qquad (4.5)$$

and

$$U_{d - {}^6Li}(R_d) = \int \{ U_{d-\alpha}(|\vec{R}_\alpha - \tfrac{1}{3}\vec{Z}|) + U_{d-d}(|\vec{R}_d + \tfrac{2}{3}\vec{Z}|) \} |\phi_o^{{}^6Li}(\vec{Z})|^2 \, d\vec{Z} \qquad (4.6)$$

The coordinates used in these equations are defined in Fig. 5. The present calculation use the α-particle-α-particle potential $U_{\alpha\alpha}$, the α-particle-deuteron potential $U_{\alpha d}$ and the deuteron-deuteron potential U_{dd} in the Woods-Saxon form with parameters given in Tab. 2.

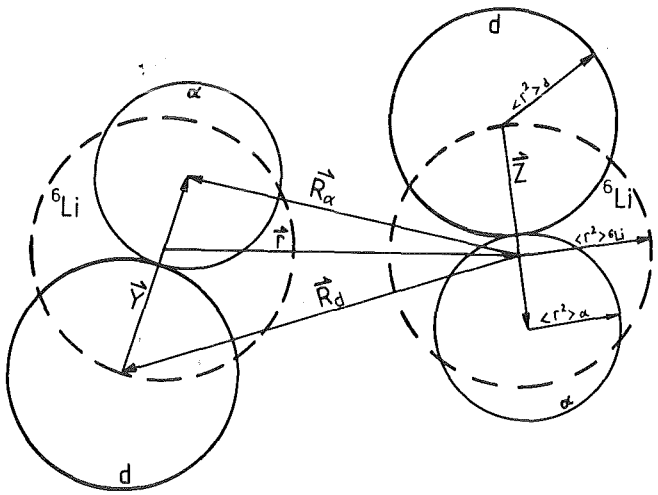

Fig. 5 Definition of the coordinate vectors used in the double-folding cluster model.

System	V_o[MeV]	r_o[fm]	a[fm]	Ref.
α - α	125.0	1.18	0.660	16
α - d	73.2	1.25	0.614	17
d - d	69.4	1.15	0.553	see text

Tab.2 Parameters of the Woods-Saxon potentials used

The d-d potential has been obtained by a standard optical model analysis of 51.5 MeV elastic deuteron-deuteron scattering data measured at the Karlsruhe Isochronous Cyclotron [18].

The cluster wave function $\phi_o^{^6Li}$ of the ^{6}Li ground state which takes into account the requirement for a shell model mode was taken from Ref. 19.

In Fig. 6 the double-folding potential (DF) and the double-folding cluster potential (DFC) are compared to the real part of the best-fit phenomenological optical potentials. In addition, interesting integral quantities (rms-radius, specific volume integrals), half-way radius $R_{1/2}$ and the (10 % - 90 %) surface thickness t are given in Tab. 3.

Applying the microscopically derived potentials for the description of the measured differential cross sections the imaginary part has to be added. Taking a WS form the parameters have been fitted together with the spin-orbit potential and a renormalization N of the strength of the real part (Tab. 4)

The factor N adjusts the strengths of the semi-microscopic potentials in such a way that the radial slopes of the potentials in the range r = 3-5 fm agree with those of the phenomenological potentials within error bars provided by the FB-method. Obviously, the experimental differential cross sections determine preferentially this (real) potential region. This observation is additionally

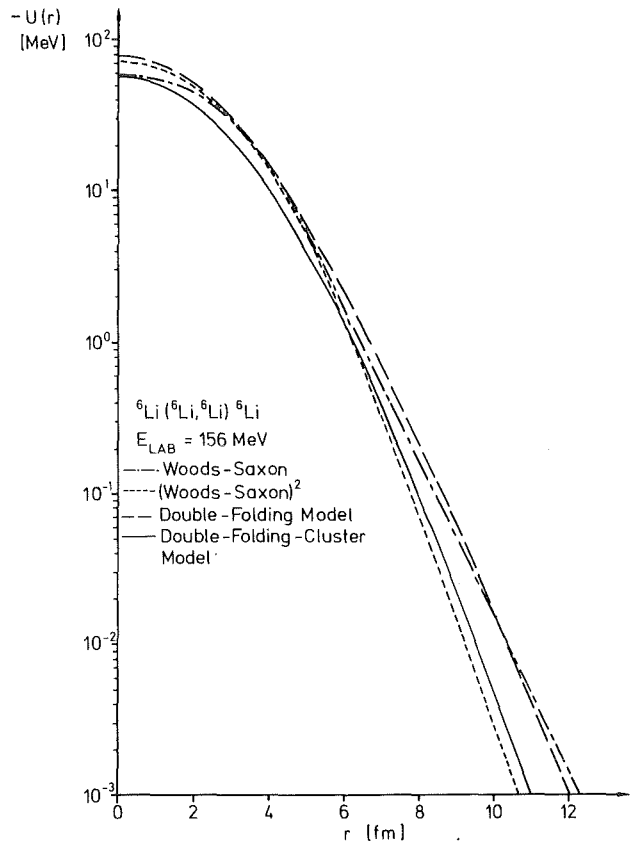

Fig. 6 Shapes of the real part of the ^{6}Li + ^{6}Li optical potential resulting from the best-fits using different radial form factors.

Potential	U(r=0) [MeV]	$\langle r^2 \rangle^{1/2}$ [fm]	$-J_V/6A$ [MeV fm^3]	$R_{1/2}$ [fm]	$t_{10} - t_{90}$ [fm]
WS	57.9	3.93	340	3.05	3.5
WS 2	71.6	3.68	325	2.67	3.8
DF	77.7	3.94	370	2.58	3.7
DFC	59.2	3.90	268	2.51	3.7
FB	62.3	3.57±0.14	385±20	3.19	3.1

Tab. 3 Integral quantities and values of some standard quantities for the real part of the ^{6}Li + ^{6}Li scattering potentials.

Proc.	N	$-W_o$ [MeV]	r_w [fm]	a_w [fm]	V_{so} [fm]	r_{so} [fm]	a_{so} [fm]	χ^2/F
DF	0.89	6.64	3.21	0.70	0.94	2.50	0.30	3.6
DFC	1.17	6.11	3.26	0.72	0.54	2.43	0.23	2.9

Tab. 4 Renormalization of the strength of the semi-microscopic potentials and best-fit parameter values of the imaginary and the spin-orbit potential

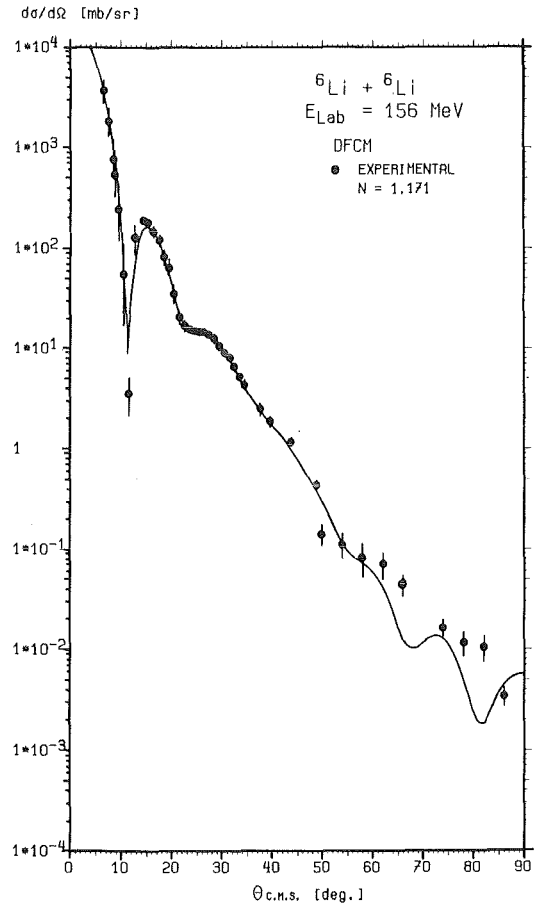

Fig. 7
Optical model description of 156 MeV ^{6}Li scattering by ^{6}Li using a double folding cluster potential (DFC) for the real part of the interaction potential

corroborated by a result of coupled channel analyses [11] including the experimental data for the inelastic ^{6}Li scattering from the 3^+_1 (E_x = 2.185 MeV) state in ^{6}Li. The resulting real potential, though somewhat different in the various parameter values of a (deformed) WS form nicely agrees in the sensitive region r=3-5 fm.

In contrast to the findings with the usual double-folding model, the calculated double-folding cluster potential underestimates the strength of the real potential. This feature may indicate some deficiencies, e.g. less proper handling of exchange and saturation effects. Though the use of a phenomenologically derived free α-α-interaction may absorb some effects of this kind, this might also overestimate the saturation of the effective interaction as α-clusters and free α-particles certainly differ due to different polarization by their nucleonic environment. In view of the fact, however, that all ingredients of the double-folding cluster model are taken from independent sources without any adjustment and refinement, and in view of the extreme assumption of complete α-d-clustering, the sucess of this model is remarkable.

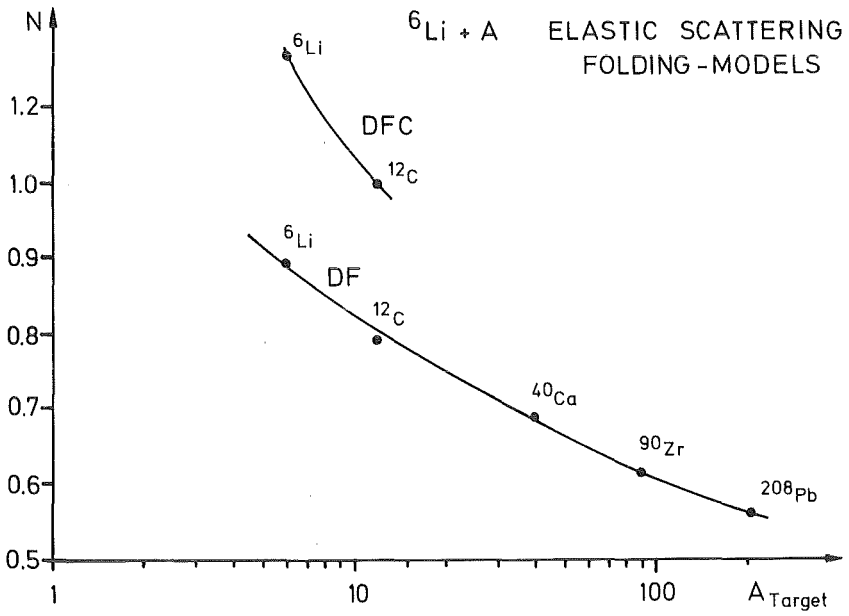

Fig. 8 A-dependence of the renormalization of the strength of the semi-microscopic potentials

Fig. 8 displays a conspicuous trend of the required renormalization of the semi-microscopic potentials (including results with heavier target nuclei [12]). Any explanation of the anomalous behaviour of the ^{6}Li projectile with respect to a folding model description should incorporate this feature.

5. Conclusions

The differential cross section for elastic scattering of 156 MeV ^{6}Li ions from ^{6}Li has been measured and analysed using various radial forms for the real part of the optical potential and taking into account the spin 1 - identical particle nature of the ^{6}Li + ^{6}Li scattering. Effects due to a spin-orbit interaction are found to be less significant within the limits of the experimental accuracy. The data determine most sensitively a restricted radial range of the real (central) potential, mainly the region beyond the half-way radius of the nuclear density in ^{6}Li. The sensitive region is also reproduced by potentials calculated on a microscopic basis and slightly adjusted in strength. A quasi model-independent analysis using the Fourier-Bessel method reveals the limits of simple phenomenological forms for the radial shape of the real interaction potential.

The success of deriving the ^{6}Li + ^{6}Li interaction from the mutual interaction of substructures both in projectile and target supports the idea that the scattering process can be fairly well understood as a superposition of the scattering of various different "bags" of nucleons, moving rather independently in the nuclear surface. As far as only the nuclear surface (beyond one-third of the central density) is involved cluster-interactions should approximate the reality better than uncorrelated nucleon-nucleon interactions [20]. This is not necessarily in contrast to the usual double-folding models using a single-nucleon-distribution as long as the cluster representation does not contradict the shell model requirements.

The continuous interest of Prof. Dr. G. Schatz in our studies is gratefully acknowledged. We thank Dr. J. Buschmann and Ing. S. Zagromski for their help in measuring the elastic scattering cross sections and Dr. D.K. Srivastava for useful comments on the problems of the analysis.

References

1) H.J. Gils, J. Buschmann, Z. Majka, B. Neumann, H. Rebel, S. Zagromski and H. Klewe-Nebenius, in Heavy ion physics ed. A. Berinde, V. Ceausescu and J.A. Dorobantu (Proc. Predeal Int. School, Romania, 1978) p. 1133

2) R.M. de Vries, D.A. Goldberg, J.W. Watson, M.S. Zisman and J.G. Cramer, Phys. Rev. Lett. 39 (1977) 450

3) G.R. Satchler and W.G. Love, Phys. Rep. 55 (1979) 183

4) V.Hnizdo, K.W. Kemper and J. Szymakowski Phys. Rev. Lett. 46 (1981) 590

5) I.J. Thompson and M.A. Nagarajan, Phys. Lett. B106 (1981) 163
R.S. Mackintosh and A.M. Kobos, Phys. Lett. B116 (1982) 95

6) Y.Sakuragi, M. Yahiro and M. Kamimura Progr. Theoret. Physics 170 (1983) 1047

7) Z. Majka, H.J. Gils, and H. Rebel, Z. Physik A288 (1978) 139

8) K. Kumar, A.K. Jain, J. Phys. Nucl. Phys. G8 (1982) 827 and references quoted therein

9) Z. Majka, H.J. Gils and H. Rebel, Phys. Rev. C25 (1982) 2996

10) E. Norbeck, P.T. Wu, C.R. Chen and T.T. Carlson, Phys. Rev. C 28 (1983) 1140
J. Cook, Atomic Data and Nuclear Data Tables 26 (1981) 19

11) S. Micek, H. Rebel and H.J. Gils, Contr. paper to the conference "Excited states in nuclei" June, 25-29, 1984, Lódz (Poland)
S. Micek, J. Buschmann, H.J. Gils, H. Klewe-Nebenius, H. Rebel and S. Zagromski (in preparation)

12) J. Cook, H.J. Gils, H. Rebel, Z. Majka and H. Klewe-Nebenius Nucl. Phys. A388 (1982) 173

13) M.D. Cokler, R.J. Griffiths, N.M. Clarke and J.S. Hanspal, J. Phys. G: Nucl. Phys. 5 (1979) L 43

14) E. Friedman and C.J. Batty, Phys. Rev. C17 (1978) 34

15) K.H. Bray, Mahavir Jain, K.S. Jayaraman, G. Lobianco, G.A. Moss, H.T.M. van Oers, D.O. Wells, F. Petrovich, Nucl. Phys. A189 (1972) 35

16. V.G. Neudatchin, V.I. Kukulin, V.L. Korotkikh and V.P. Korennay, Phys. Lett. 34B (1971), 581

17) F. Hinterberger, G. Mairle, U. Schmidt-Rohr, G.J. Wagner, Nucl. Phys. A111 (1968) 265

18) H. Brückmann, E.L. Haase, W. Kluge, L. Schänzler, Z. Physik 230 (1970) 383

19) V.G. Neudatchin, Proc. Int. Conf. on Clustering Phenomena in Nuclei, Bochum, July 1969 (IAEA, Vienna) (1969). I.V. Kurdyumov, V.G. Neudatchin, and Yu.F. Smirnov, Phys. Lett. 31B, 426 (1970).

20) D.M. Brink and J.J. Castro, Nucl. Phys. A216 (1973) 109